# A LATTICE GAS MODEL OF ELECTROCHEMICAL CELLS : MEAN-FIELD KINETIC APPROACH

M.-O. BERNARD, M. PLAPP, J.-F. GOUYET
*Laboratoire de Physique de la Matière Condensée,*
*Ecole Polytechnique, F-91128 Palaiseau, France*
*E-mail: jean-francois.gouyet@polytechnique.fr*

The present work is an attempt to simulate electrochemical cells and growth structures that form during electrodeposition. For that purpose we use a lattice gas model with charged particles, and build mean-field kinetic equations for their evolution, together with a Poisson equation for the electric potential, and oxido-reduction reactions on the electrode surfaces for the growth. In this preliminary study we confirm the viability of this approach by simulating the ion kinetics in front of planar electrodes during growth and dissolution.

## 1 Introduction

Electrochemical phenomena are ubiquitous in nature, and of particular industrial importance. They play a basic role in batteries, corrosion problems, electrodeposition of parts and circuitry, as well as in biochemical reactions. Electrochemical growth may lead to the formation of complex and highly branched structures that can be fractals or densely branched, depending on the experimental conditions[1,2,3,4]. Figure 1 shows an example of a fractal growth structure. While diffusion-limited aggregation (DLA)[5] and similar models produce structures that are strikingly similar to such experimental pictures, they greatly simplify the underlying phenomena and can hence not yield detailed information on the relation between growth conditions and characteristics of the growth structures such as growth speed, branch thickness and overall structure.


Figure 1. Electrodeposition of copper on a substrate (reprinted with permission from V. Fleury). The quasi-two-dimensional cell is composed of two copper electrodes and a $CuSO_4$ solution for the electrolyte (sample size $3 \times 2\,\mathrm{mm}^2$). Only a small part of the sample is shown.

To obtain such information, the motion of charged particles as well as their pro-

duction/consumption by chemical reactions have to be taken into account. Despite the fact that charged systems are everywhere around and in us, many questions remain open. The main difficulty comes from the coexistence of competing short-range Van der Waals or chemical interactions, and long-range Coulomb interactions. Our aim is to simulate at least qualitatively in two dimensions electrochemical growth leading to branched structures such as observed experimentally[1,2,3,4].

For that purpose, we use a lattice gas model that includes charged particles and uses simple microscopic transformation rules to simulate the salient features of the electrochemical process, including both the diffusion kinetics of the charged and neutral species, and the oxido-reduction phenomena on the electrode interfaces. There exist, to our knowledge, no theoretical studies of the behavior of an entire electrochemical cell based on a microscopic model; lattice gas models have been used to simulate phenomena located on the electrode surfaces, such as adsorption or underpotential deposition[6], and for studies of ionic transport at liquid-liquid interfaces[7]. Marshall and Mocskos [8] have combined a lattice model for the electrodes and a continuum treatment for the electrolyte to simulate ramified growth; however, in this approach the detailed description of the interface is lost. While our model still contains strong simplifications, it provides a consistent description of the whole cell and is much closer to the basic microscopic physics and chemistry than the original DLA model and its generalizations that use, for example, a uniform drift to simulate the effect of the electric field [9].

To investigate the dynamics of the model, we will extend the formalism of Mean-Field-Kinetic-Equations (MFKE)[10,11,12] that has been used to study numerous transport and growth phenomena in alloys, including diffusion and ordering kinetics, spinodal decomposition and dendritic growth[?,14,15]. To describe electrodeposition, we need to include charged particles. This implies that, in addition to the kinetic equations driving the particle motion, we have to solve the Poisson equation that determines the local electrical potential. The chemical potentials present in the MFKE are then replaced by electrochemical potentials. In this way, the present method is able to establish a link between a microscopic lattice model and macroscopic phenomenological equations[16,17]. We present here some results on the growth and dissolution of planar electrodes in a binary electrolyte that are in good qualitative agreement with the macroscopic model of Chazalviel[17]. Finally, we report preliminary two-dimensional simulations that exhibit fingered growth structures.

## 2 Model

We consider an electrochemical cell, composed of a binary electrolyte and two metallic electrodes. The absence of supporting electrolyte, generally used to suppress ion migration, corresponds here to the experimental situation in Fig. 1. To take into account the crystalline structure of the electrodes, they are modeled by a lattice, whose sites are occupied by metallic atoms. It is then convenient to represent the electrolyte by the same lattice, occupied by a solvent, and by cations and anions. We consider a two-dimensional lattice gas on a square lattice with lattice spacing $a$. The cations $M^+$ give metallic atoms $M^0$ after reduction, and the anions $A^-$ are considered to be non reactive. Their presence ensures the electroneutrality of the

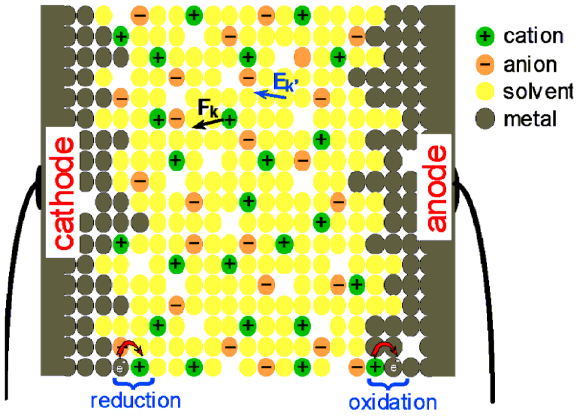


Figure 2. The lattice gas model used in the present study. A fixed potential difference is imposed across the electrodes. The ions in the electrolyte are submitted to an electric field $\mathbf{E_k}$ (and a force $\mathbf{F_k} = q\mathbf{E_k}$) at their lattice site position $\mathbf{k}$. The various species have short range interactions (in the present work, attractive interactions are considered between solvent and ions, solvent and solvent, and metal and metal). Oxido-reduction reactions appear on the electrode interfaces.

solution at equilibrium. The solvent $S$ is neutral, but can interact through short range interactions with the other species. For simplicity, the two electrodes are supposed to consist of the same metal, as is the case in the experiment of Fig. 1. We suppose steric exclusion between the different species, i.e. a given site can be occupied by only one species or it can be empty. The diffusion processes are mediated by a small number of vacancies, i.e. a species is allowed to jump onto a neighboring empty site (using an exchange process between nearest neighbor species would also be possible, but is more complicated to implement). To model short-range interactions, we introduce nearest neighbor attractive interactions on the lattice. In addition, we have long range Coulomb interactions between the charged species. We must, in addition, consider electrons in the metallic electrodes: they have a particular status that will be discussed later.

The establishment of the Mean-Field-Kinetic-Equations (MFKE) follows the same procedure as for neutral particles[10,11,12]. We first write the Boolean kinetic equations on the lattice, starting from the general master equation,

$$\frac{\partial}{\partial t}P(\{n\},t) = \sum_{\{n'\}} \left[W(\{n'\} \to \{n\})P(\{n'\},t) - W(\{n\} \to \{n'\})P(\{n\},t)\right] , \quad (1)$$

which gives the probability $P$ to find at time $t$ a given configuration $\{n\}$, that is the occupation of each site by one of the species $\alpha = M^0, M^+, A^-, S$ or by a vacancy $v$. $\{n\}$ is the set of the occupation numbers $n^\alpha_{\mathbf{k}}$ on each site $\mathbf{k}$ of the lattice ($n^\alpha_{\mathbf{k}} = 1$ if $\mathbf{k}$ is occupied by species $\alpha$ and 0 otherwise). Double occupancy exclusion imposes

$$\sum_\alpha n^\alpha_{\mathbf{k}} + n^v_{\mathbf{k}} = 1 . \quad (2)$$

$W(\{n\} \to \{n'\})$ is the probability per unit time that configuration $\{n\}$ is changed

into configuration $\{n'\}$. During the process $\{n\} \to \{n'\}$, one particle (metal, ion, or solvent) jumps to one of its vacant nearest neighbor sites. The jump probability depends not only on the local interactions with their neighborhood, but for the charged species also on the local electric field.

In the present work, we will be interested in the time evolution of the average concentrations of the various species ($\alpha = +, -, 0, S, v$),

$$p_{\mathbf{k}}^{\alpha} = \langle n_{\mathbf{k}}^{\alpha} \rangle = \sum_{\{n\}} n_{\mathbf{k}}^{\alpha} P(\{n\}, t). \tag{3}$$

In addition, we define $p_{\mathbf{k}}^{e}$ as the excess electron concentration on site $\mathbf{k}$ (that is, the difference between the actual number of electrons and the equilibrium number for a metal concentration $p_{\mathbf{k}}^{0}$, see below). The short range (attractive) interaction between two species $\alpha$ and $\beta$ is limited to nearest neighbors and noted $\epsilon^{\alpha\beta}$. But in principle any longer range attractive or repulsive interaction can be considered. The temperature is fixed and constant in the whole system, and the external control parameter is the potential difference $\Delta V$ applied across the cell.

## 3 Mean-Field Kinetic and Poisson Equations

To establish the Mean-field-Kinetic-Equations, we follow the lines described in previous papers concerning spinodal decomposition, ordering or dendritic growth[12,13,14]. Two important new elements appear: *a*) there is an electric potential related to the charge distribution, and *b*) oxidation and reduction may take place at the electrodes.

### *3.1 Kinetic equations of the particles*

The local concentration of the species $M^0$ and $M^+$ is modified by transport (diffusion and migration in the electric field) and by the chemical reaction; for the other species $A^-$ and $S$, only transport is present. The MFKE derived from the microscopic model read

$$\frac{\partial p_{\mathbf{k}}^{+}}{\partial t} = -\sum_{\mathbf{a}} \widetilde{J}_{\mathbf{k},\mathbf{k}+\mathbf{a}}^{+} - \sum_{\mathbf{a}} \sigma_{\mathbf{k},\mathbf{k}+\mathbf{a}}, \tag{4}$$

$$\frac{\partial p_{\mathbf{k}}^{0}}{\partial t} = -\sum_{\mathbf{a}} \widetilde{J}_{\mathbf{k},\mathbf{k}+\mathbf{a}}^{0} + \sum_{\mathbf{a}} \sigma_{\mathbf{k},\mathbf{k}+\mathbf{a}}, \tag{5}$$

$$\frac{\partial p_{\mathbf{k}}^{-}}{\partial t} = -\sum_{\mathbf{a}} \widetilde{J}_{\mathbf{k},\mathbf{k}+\mathbf{a}}^{-}, \tag{6}$$

$$\frac{\partial p_{\mathbf{k}}^{s}}{\partial t} = -\sum_{\mathbf{a}} \widetilde{J}_{\mathbf{k},\mathbf{k}+\mathbf{a}}^{s}. \tag{7}$$

Here, $\widetilde{J}^{\alpha}_{\mathbf{k},\mathbf{k+a}}$ is the diffusion current of species $\alpha$ on the bond linking site $\mathbf{k}$ to its nearest neighbor site $\mathbf{k}+\mathbf{a}$. Generalizing previous studies[10,11,12,15] to the electrochemical case, we can write this current as the product of a bond mobility $\widetilde{M}^{\alpha}_{\mathbf{ij}}$ times the (discrete) gradient of an electrochemical potential $\widetilde{\mu}^{\alpha}_{\mathbf{i}}$,

$$\widetilde{J}^{\alpha}_{\mathbf{k},\mathbf{k+a}} = -\widetilde{M}^{\alpha}_{\mathbf{k},\mathbf{k+a}} \mathfrak{D}_{\mathbf{a}} \widetilde{\mu}^{\alpha}_{\mathbf{k}}\,, \tag{8}$$

where $\mathfrak{D}_{\mathbf{a}}$ is a difference operator acting on the site coordinates, $\mathfrak{D}_{\mathbf{a}} f_{\mathbf{k}} = f_{\mathbf{k+a}} - f_{\mathbf{k}}$. The electrochemical potential,

$$\widetilde{\mu}^{\alpha}_{\mathbf{k}} = \mu^{\alpha}_{\mathbf{k}} + q^{\alpha} V_{\mathbf{k}} = -\sum_{\beta}\sum_{\mathbf{a}} \varepsilon^{\alpha\beta} p^{\beta}_{\mathbf{k+a}} + kT \ln\left(\frac{p^{\alpha}_{\mathbf{k}}}{p^{v}_{\mathbf{k}}}\right) + q^{\alpha} V_{\mathbf{k}}, \tag{9}$$

is the sum of three contributions: a local energy due to the interaction of species $\alpha$ with its local environment, an entropy term (these two constitute the chemical potential $\mu^{\alpha}_{\mathbf{k}}$), and an electrostatic energy ($V_{\mathbf{k}}$ is the electrostatic potential at site $\mathbf{k}$, and $q^{\alpha}$ is the electric charge of species $\alpha$). The presence of the vacancy concentration in the denominator of the entropic contributions comes from the constraint of Eq. (2). The mobility along a bond **i -j** is given by (see an analogous case, in the absence of electric charges[20]),

$$\widetilde{M}^{\alpha}_{\mathbf{k},\mathbf{k+a}} = \frac{w^{\alpha}}{kT} p^{v}_{\mathbf{k}} p^{v}_{\mathbf{k+a}} \exp\frac{(\widetilde{\mu}^{\alpha}_{\mathbf{k}} + \widetilde{\mu}^{\alpha}_{\mathbf{k+a}})}{2kT} \mathrm{shc}\frac{(\widetilde{\mu}^{\alpha}_{\mathbf{k+a}} - \widetilde{\mu}^{\alpha}_{\mathbf{k}})}{2kT}\,, \tag{10}$$

where we have used the notation $\mathrm{shc}u = \sinh u/u$ (close to equilibrium, $\widetilde{\mu}^{\alpha}_{\mathbf{k+a}} \cong \widetilde{\mu}^{\alpha}_{\mathbf{k}}$ and $\mathrm{shc}\left[(\widetilde{\mu}^{\alpha}_{\mathbf{k+a}} - \widetilde{\mu}^{\alpha}_{\mathbf{k}})/kT\right] \cong 1$).

Finally, $\sigma_{\mathbf{k},\mathbf{k+a}}$ is the current of electronic charges from $\mathbf{k}+\mathbf{a}$ to $\mathbf{k}$ (current of positive charges from $\mathbf{k}$ to $\mathbf{k}+\mathbf{a}$) reducing the cations on site $\mathbf{k}$ (resp. electronic current issued from the oxidation of the metal) via a corresponding elimination (resp. creation) of electrons on site $\mathbf{k}+\mathbf{a}$,

$$M^{+}(\mathbf{k}) + e^{-}(\mathbf{k}+\mathbf{a}) \rightleftharpoons M^{0}(\mathbf{k}). \tag{11}$$

The direction of the reaction depends on the relative magnitude of the electrochemical potentials of the involved species. Reduction of cations on a site $\mathbf{k}$ of the cathode appears when

$$\widetilde{\mu}^{+}_{\mathbf{k}} + \widetilde{\mu}^{e}_{\mathbf{k+a}} > \widetilde{\mu}^{0}_{\mathbf{k}}; \tag{12}$$

otherwise, the metal is oxidized. The reduction rate on site $\mathbf{k}$ is the sum of all the reaction paths $\sum_{\mathbf{a}} \sigma_{\mathbf{k},\mathbf{k+a}}$. Following[18], we can write the reaction rate,

$$\sigma_{\mathbf{k},\mathbf{k+a}} = w^{*}_{\mathbf{k},\mathbf{k+a}} \left(\exp\frac{\widetilde{\mu}^{+}_{\mathbf{k}} + \widetilde{\mu}^{e}_{\mathbf{k+a}}}{kT} - \exp\frac{\widetilde{\mu}^{0}_{\mathbf{k}}}{kT}\right) \tag{13}$$

The coefficient $w^{*}_{\mathbf{k},\mathbf{k+a}}$ is determined by comparison with the mesoscopic theory of Butler-Volmer and corresponds to the electronic tunneling from the metal surface to the nearest neighboring cation; $\widetilde{\mu}^{e}_{\mathbf{k}}$ is the local chemical potential of the electrons (for the definitions of both quantities, see below).

*3.2 The Poisson problem*

To determine the electrostatic potential for a given charge distribution, we solve a discrete version of the Poisson equation using the lowest order discretization for the Laplacian that involves only nearest neighbor sites,

$$-4V_{\mathbf{k}} + \sum_{\mathbf{a}} V_{\mathbf{k}+\mathbf{a}} = -\frac{a^{2-d}}{\epsilon} \sum_{\alpha=+,-,e} q^{\alpha} p^{\alpha}_{\mathbf{k}} \tag{14}$$

where $\epsilon$ is the permittivity (for simplicity, the same for all species), and $q^{\alpha}$ the charge of species $\alpha$ ($q^e = -e$, for the electrons); $a$ is the lattice spacing and $d$ the spatial dimension.

The boundary conditions at the metal-electrolyte interface have to be considered with special care. In a "macroscopic" picture where this interface is of arbitrary form but sharp (i.e. represented by a mathematical line), the electric field is zero in the metal, and the potential is constant and equal to the imposed boundary condition up to the sharp interface. If there is an electric field in the electrolyte, surface charges are created. In the mean-field representation outlined above, the interface is diffuse, i.e. "smeared out" over several lattice sites, and both the definition of the boundary condition and the creation of surface charges have to be consistently implemented. We solve these problems by the introduction of very mobile electrons diffusing from site to site in the metal, and solve the Poisson equation for all the charges, including electrons. More precisely, we denote by $p^e{}_{\mathbf{k}}$ the deviation from the neutral state expressed in electrons per site. Hence, $p^e{}_{\mathbf{k}} > 0$ corresponds to an excess of electrons, $p^e{}_{\mathbf{k}} < 0$ to an electron deficit. Their chemical potential is defined by

$$\widetilde{\mu}^e_{\mathbf{k}} = E_F + q^e V_{\mathbf{k}} + \frac{p^e{}_{\mathbf{k}}}{\mathcal{D}(E_F)} \tag{15}$$

where $q^e = -e$, $E_F$ is the Fermi level of the metal, and $\mathcal{D}(E_F)$ is the density of electronic states at the Fermi level. This corresponds to screening in the Thomas-Fermi approximation[19]. The electronic current is then

$$\widetilde{J}^e_{\mathbf{k},\mathbf{k}+\mathbf{a}} = -\widetilde{M}^e_{\mathbf{k},\mathbf{k}+\mathbf{a}} \mathfrak{D}_{\mathbf{a}} \widetilde{\mu}^e_{\mathbf{k}} \tag{16}$$

and the time evolution of the excess electron concentration is

$$\frac{\partial p^e_{\mathbf{k}}}{\partial t} = -\sum_{\mathbf{a}} \widetilde{J}^e_{\mathbf{k},\mathbf{k}+\mathbf{a}} - \sum_{\mathbf{a}} \sigma_{\mathbf{k}+\mathbf{a},\mathbf{k}} \tag{17}$$

where the last term is the reaction term, active only in the solid-electrolyte interface. To force the electrons to stay in the metallic regions, we write the mobility in the form,

$$\widetilde{M}^e_{\mathbf{k},\mathbf{k}+\mathbf{a}} = \frac{w^e}{kT} f(p^0_{\mathbf{k}}) f(p^0_{\mathbf{k}+\mathbf{a}}) \tag{18}$$

where $f$ is chosen important only if the metallic concentration is large enough. In particular, the rough surface, with a lower mean concentration, will present a low electronic mobility. We have used for $f$ a monotonous function varying from 0 when

$p = 0$, to 1 for $p = 1$, with a rapid variation around some concentration $p_c$ that is reminiscent of some percolation threshold. A convenient choice is,

$$f(p) = \frac{\tanh[(p - p_c)/\xi] + \tanh[p_c/\xi]}{\tanh[(1 - p_c)/\xi] + \tanh[p_c/\xi]}. \tag{19}$$

where $\xi$ is of the order of the interface thickness.

The above expressions are chosen such that the excess of electrons will be localized in the interface. This model provides a fast way to calculate the surface charges on the electrodes. In practice, to save computational time we impose a fixed potential value inside both electrodes up to a given distance from the interfaces, which reduces the diffusion time of the electrons from the source to the surface where they are involved in the chemical reaction.

The interpolation function $f(p)$ is also used to specify the prefactor $w^*_{\mathbf{k},\mathbf{k}+\mathbf{a}}$ of the reaction rate (eq. 13),

$$w^*_{\mathbf{k},\mathbf{k}+\mathbf{a}} = w^* \left(1 - f(p^0_{\mathbf{k}})\right) f(p^0_{\mathbf{k}+\mathbf{a}}) \, . \tag{20}$$

In this way, the transfer is localized around the metal-electrolyte interface, where occupied metallic sites and electrolyte sites are neighbors. $w^e$ in eq. 18 and $w^*$ in eq. 20 are constant frequency factors.

## 4 Simulations

The first step, before considering two-dimensional cells in which electrodeposition creates dendritic patterns, is to check if one-dimensional systems work correctly. We have performed calculations on 200-site cells. The two electrodes are identical, with a thickness of 40 layers. The initial system is neutral everywhere: anion and cation concentrations are taken equal and there are no electrons in excess. We have chosen, in addition to the Coulomb interactions, attractive interactions between the solvent and anions, cations, and itself, as well as between metallic atoms: $\varepsilon^{s+} = \varepsilon^{s-} = \varepsilon^{ss} = \varepsilon^{00} = 1$, with the choice $kT = 1$, all the other interactions being zero[a]. The initial concentrations of each species are chosen such that the system is in equilibrium in the absence of an applied potential. This corresponds to a uniform chemical potential for each species. The various parameters that control the relative importance of the diffusion and reaction processes are chosen as follows:

- Initial concentrations :

$$\begin{array}{ll} p^0_{electrodes} = 0.925, & p^0_{electrolyte} = 0.0025 \\ p^{\pm}_{electrodes} = 3 \times 10^{-4}, & p^{\pm}_{electrolyte} = 0.01 \\ p^s_{electrodes} = 0.0025, & p^s_{electrolyte} = 0.907 \end{array}$$

- Jump frequencies : $w^\alpha = 1$, for $\alpha = +, -, 0, s$; and $w^e = 10^{-3}$, for the electrons (the electron mobility remains nevertheless faster than the mobility of the other species).

[a] The problem is oversimplified for the electrodes as it is known that quantum effects are important in the interaction between metallic atoms, and do not reduce to simple nearest neighbor interactions. This has no strong consequences for the present study.

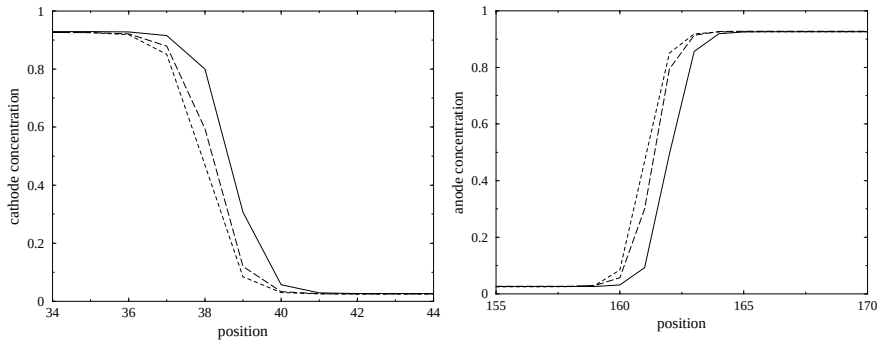


Figure 3. Picture showing the dissolution of metal at the anode (on the right), and the electrodeposition (reduction) at the cathode (on the left), at times $t = 0$ (dotted line), $t = 0.5 \times 10^5$ (dashed line), and $t = 5 \times 10^5$ (solid line). The last time corresponds to one monolayer of metal dissolved or deposited.

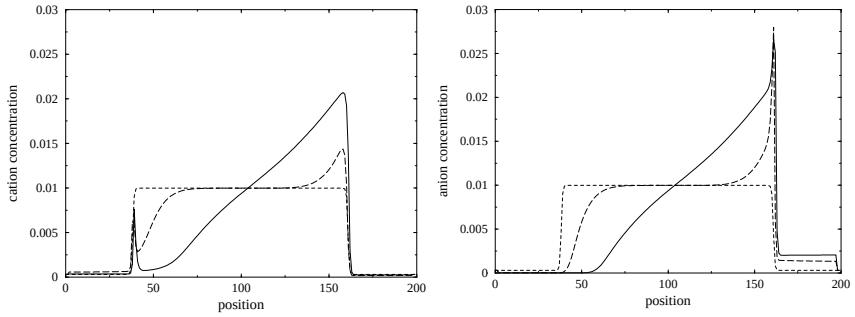


Figure 4. Cation (left) and anion (right) concentration profiles at times $t = 0$ (dotted line), $t = 0.5 \times 10^5$ (dashed line), $t = 5 \times 10^5$ (solid line).

- Transfer frequency : $w^* = 10^{-5}$; Fermi energy : $E_F/kT = 4.42$; density of states at the Fermi level: $\mathcal{D}(E_F) = 1000/kT$.
- Electrical parameters : $q^{\pm} = \pm e; q^e = -e$; $e = 1$; (dimensionless) permittivity: $\epsilon = 5 \times 10^{-2}$; applied potential difference : $10kT/e$.

When a potential is applied, the ionic species start to migrate, double layers appear on the interfaces, reduction processes take place on the cathode, and oxidation processes on the anode. Figure 3 shows the growth of the cathode and the dissolution of the anode. We notice that the shape of the metal concentration profile across the interface is essentially preserved, and that the deposited metal has the same concentration as the initial electrode.

The interesting results concern the kinetics of the ions. In Fig.4 that shows the evolution of the ion concentrations, we observe the progressive formation of a concentration gradient between the anode and the cathode with, for the cations, a concentration peak on the cathode (accompanied by an electronic layer on the

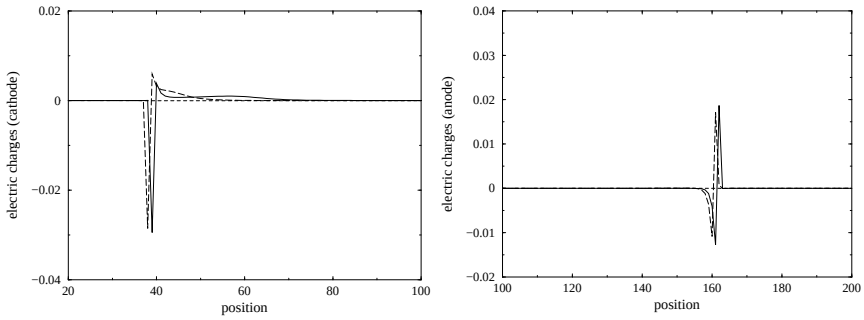


Figure 5. Charge distribution at times $t = 0.5 \times 10^5$ (dashed line) and $t = 5 \times 10^5$ (solid line). In addition to the double layers close to the interfaces, there is an extended space charge in front of the cathode as found by Chazalviel [17].

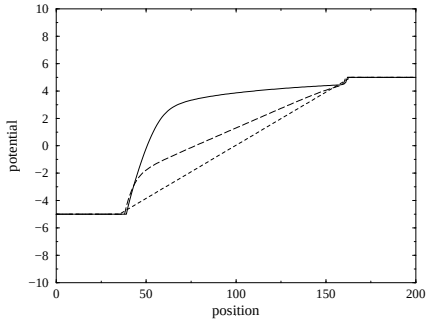


Figure 6. Potential profiles at times $t = 0$ (dotted line), $t = 0.5 \times 10^5$ (dashed line), $t = 5 \times 10^5$ (solid line).

metal surface). The anion concentration profile presents on the contrary an increase close to the anode.

Figure 5 shows the total charge distribution at two successive times, where we can see, in addition to the double-layers located around the interfaces, an excess of cations over the anions, on a range of about 30 lattice distances. This extended space charge leads to an important potential drop on the cathode side, as can be seen in Fig. 6 that shows the electric potential. In summary, the electrolyte domain can be divided into four regions that can be clearly distinguished at times larger than $t = 5 \times 10^5$ steps: the double layers very close to the interfaces, an almost electroneutral region where the concentration gradients are approximately constant, and the ion-depleted space charge region close to the cathode. According to Chazalviel[17], this extended space charge is crucial for the emergence of ramified growth: the strong electric field close to the surface leads to a Laplacian instability of a flat front, and the one-dimensional calculation becomes invalid.

## 5 Two-dimensional simulations: dendritic growth

We present now preliminary simulations of two-dimensional samples. We use a $100 \times 40$ sample with the same parameters as in the preceding one-dimensional simulations, except for the potential difference ($100kT/e$, corresponding to $\Delta V \approx 2.5$ V at room temperature), the transport frequency ($\omega^* = 6 \times 10^{-3}$) and the metal jump frequency ($\omega^0 = 10^{-3}$).

The geometry of the growth appears to be very sensitive to several of the model parameters, in particular to the applied voltage and the ratio of transfer frequency and metal jump frequency. In figure 7, we observe an increase of the cation concentration in front of the growing dendrite that induces a subsequent tip-splitting; for slightly different parameters, this event happens much later. A more detailed investigation is needed to elucidate the tip-splitting mechanism and the precise role of the various parameters. Also, in the present study, due to the small size of the sample, the gradients in front of the dendrites strongly depend on time. At the end, when the tips approach the anode and the gradients become very strong, the dendrite exhibits an anomalous behavior, characterized by a weakly connected growth and low metal concentration.

## 6 Conclusion

We have shown in this preliminary study that it is possible to build Electrochemical-Mean-Field-Kinetic Equations (EMFKE) that are able to reproduce qualitatively the behavior of electrochemical cells with planar electrodes. Our model leads naturally to the formation of the extended space charge, in addition to the Helmholtz double layers. This extended space charge is known to play a crucial role in the selection of the growth velocity and the dense branching structure of the deposit[4]. Furthermore, we have shown that our model leads to the emergence of dendritic growth in two-dimensional simulations.

The above EMFKE contain all the ingredients necessary to simulate dendritic growth by electrodeposition in two and three dimensions. We expect the crystalline anisotropy to be conveniently simulated by the intrinsic lattice anisotropy as in previous work on alloys[15,20]. It should be emphasized, however, that several limitations of the model have to be overcome to achieve a more quantitative modeling. Most seriously, lattice gas models cannot manage the very different length scales present in electrochemical cells, that range from the interatomic distance (Å), the capillary length that describes the effect of surface tension (of the order of the interface thickness, around 1nm), the Debye length (a few nanometers), the diffusion length (a few hundred $\mu$m), up to the cell size of a few millimeters. Since the lattice gas model explicitly contains the interatomic distance, the available computational resources do not allow to treat correctly all these scales at the same time, and the results must remain qualitative. Some of these problems could be resolved by adapting the more phenomenological phase-field method[21] to electrochemical systems and by using modern multi-scale algorithms; however, in such approaches, the direct microscopic interpretation is lost. Finally, we have ignored here the hydrodynamic convection currents that, at least in thick enough cells, play an important role in

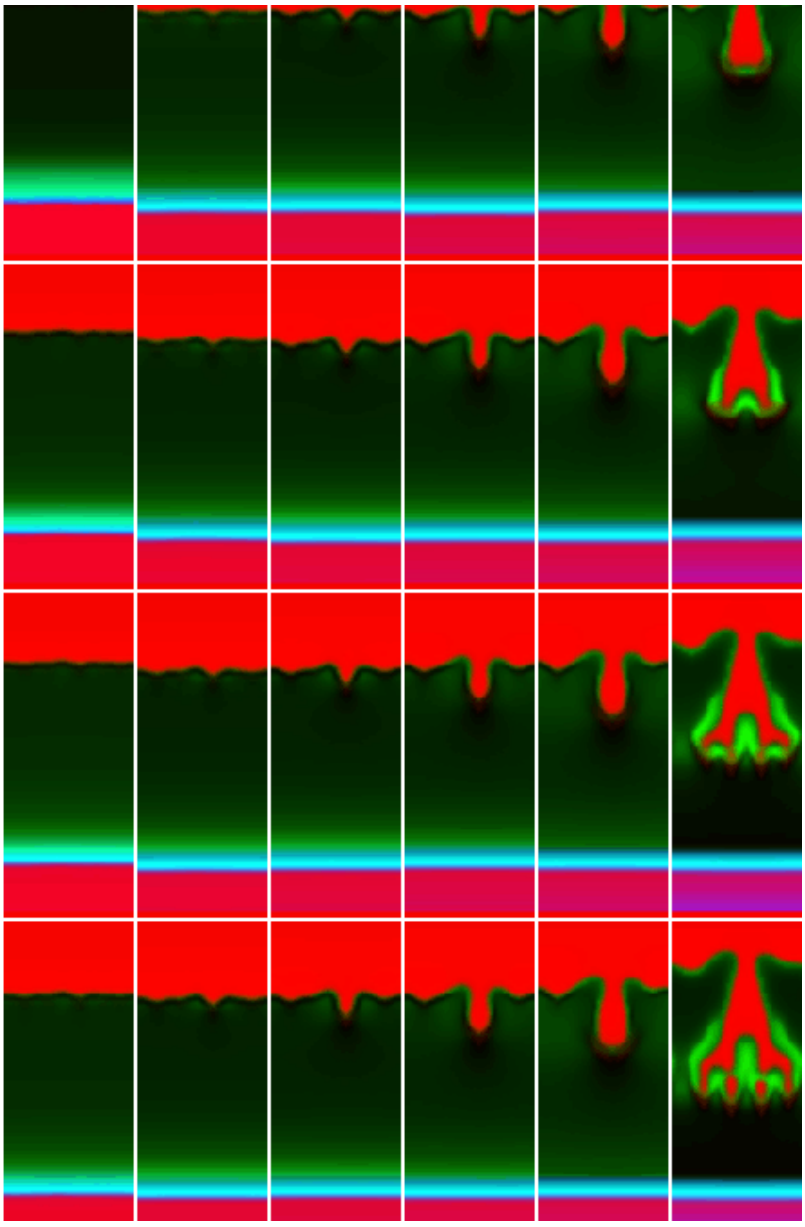

Figure 7. Evolution of a $100 \times 40$ electrochemical cell. The applied potential corresponds to $\Delta V = 2.5$ Volts. The cathode is on top, and growth precedes downwards. The concentrations of metal, anions, and cations are coded in red, green, and blue, respectively, and the cation and anion concentrations are re-scaled from approximately $8 \times 10^{-2}$ to 1 to be visible. Time evolves from top left to bottom right, by columns. Dendrites grow on the cathode, while the anode is progressively dissolved (the images are re-centered during the evolution).

the pattern selection. This convection could be included in the future, for example by using a combination of stochastic and hydrodynamical lattice-gas models.

Discussions with J.-N. Chazalviel, V. Fleury, and M. Rosso are greatly acknowledged. Laboratoire de Physique de la Matière Condensée is Unité Mixte 7643 of CNRS and Ecole Polytechnique.

## References

1. M. Matsushita, M. Sano, Y. Hayakawa, H. Honjo, and Y. Sawada, *Phys. Rev. Lett.*, **53**, 286 (1984).
2. D. Grier, E. Ben-Jacob, R. Clarke, and L.M. Sander, *Phys. Rev. Lett.*, **56**, 1264 (1986).
3. Y. Sawada, A. Dougherty, and J.P. Gollub, *Phys. Rev. Lett.*, **56**, 1260 (1986).
4. V. Fleury, M. Rosso, J.-N. Chazalviel, and B. Sapoval, *Phys. Rev. A*, **44**, 6693 (1991).
5. T. A. Witten and L. M. Sander, *Phys. Rev. Lett.*, **47**, 1400 (1981); *Phys. Rev. B*, **27**, 5686 (1983).
6. P.A. Rikvold, G. Brown, M.A. Novotny, and A. Wieckowski, *Colloids and Surfaces A: Physicochemical and Engineering Aspects ,* **134**, 3 (1998).
7. W. Schmickler, *J. Electroanal. Chem.*, **460,** 144 (1999).
8. G. Marshall, and P. Mocskos, *Phys. Rev. E*, **55**, 549 (1997)
9. S.C. Hill, and J.I.D. Alexander *Phys. Rev. E*, **56**, 4317 (1997).
10. G. Martin, *Phys. Rev. B*, **41**, 2279 (1990).
11. J.-F. Gouyet, *Europhys. Lett.*, **21** , 335 (1993).
12. V. Vaks, and S.Beiden, *Sov. Phys. JETP*, **78**, 546 (1994).
13. J.-F. Gouyet, *Phys. Rev. E*, **51**, 1695 (1995).
14. V. Dobretsov, V. Vaks, and G. Martin, *Phys. Rev. B* , **54**, 3227 (1996).
15. M. Plapp and J.-F. Gouyet, *Phys. Rev. E*, **55**, 45 (1997).
16. J.S. Kirkaldy, *Can. J. Phys.*, **57**, 717 (1979).
17. J.-N. Chazalviel, *Phys. Rev. A*, **42**, 7355 (1990).
18. W. Schmickler, *Interfacial Electrochemistry*, Oxford University Press, (1996), pages 58-63.
19. J.-N. Chazalviel, *Coulomb Screening by Mobile Charges* , Birkhäuser (1999), pages 22-27.
20. M. Plapp and J.-F. Gouyet, *Phys. Rev. Lett.*, **78**, 4970 (1997); *Eur. Phys. J. B*, **9**, 267 (1999).
21. A. Karma and W.-J. Rappel, *Phys. Rev. E*, **57**, 4323 (1998).